

Depolarization, intracellular calcium and exocytosis in single vertebrate nerve endings

Manfred Lindau,* Edward L. Stuenkel[†], Jean J. Nordmann[§]

*Biophysics Group, Freie Universität Berlin, Arnimallee 14, D-1000 Berlin 33, Germany; [†]Department of Physiology, University of Michigan, Ann Arbor, MI 48109 USA; and [§]Centre de Neurochimie, 5 rue Blaise Pascal, F-67084 Strasbourg, France

ABSTRACT We have investigated the temporal relationship between depolarization, elevation of $[Ca^{2+}]_i$ and exocytosis in single vertebrate neuroendocrine nerve terminals. The change of $[Ca^{2+}]_i$ and vasopressin release were measured with a time resolution of < 1 s in response to K^+ -induced depolarization. Exocytosis was also monitored in the whole-terminal patch-clamp configuration by time resolved capacitance measurements while $[Ca^{2+}]_i$ was simultaneously followed by fura-2 fluorescence measurements. In intact as well as patch-clamped nerve terminals sustained depolarization leads to a sustained rise of $[Ca^{2+}]_i$. The rate of vasopressin release from intact nerve terminals rises in parallel with $[Ca^{2+}]_i$ but then declines rapidly towards basal ($t_{1/2} \sim 15$ s) despite the maintained high $[Ca^{2+}]_i$, indicating that only a limited number of exocytotic vesicles can be released. We demonstrate that in nerve terminals exocytosis can be followed during step depolarization by capacitance measurements. The capacitance increase starts instantaneously whereas $[Ca^{2+}]_i$ rises with a half time of several hundred milliseconds. An instantaneous steep capacitance increase is followed by a slow increase with a slope of 25–50 fF/s indicating the sequential fusion of predocked and cytoplasmic vesicles. During depolarization the capacitance slope declines to zero with a similar time course as the vasopressin release indicating a decrease in exocytotic activity. Depolarization per se in the absence of a sufficient rise of $[Ca^{2+}]_i$ does not induce exocytosis but elevation of $[Ca^{2+}]_i$ in the absence of depolarization is as effective as in its presence. The experiments suggest that a rapid rise of $[Ca^{2+}]_i$ in a narrow region beneath the plasma membrane induces a burst of exocytotic activity preceding the elevation of bulk $[Ca^{2+}]_i$ in the whole nerve terminal.

INTRODUCTION

Nerve terminals of the posterior pituitary release vasopressin (AVP) and oxytocin upon electrical stimulation which induces the opening of voltage dependent calcium channels (Dayanithi et al., 1988; Lemos and Nowycky, 1989). In accordance with the Ca^{2+} hypothesis the entry of calcium leads to an increase of $[Ca^{2+}]_i$ which is believed to drive, by yet unknown mechanisms, the exocytotic fusion of secretory granules with the plasma membrane of the nerve terminal. An extensive literature has established the general relationship between a rise in $[Ca^{2+}]_i$ and induction of exocytosis in excitable cells with the relationship most quantitatively examined at the giant synapse of the squid (Augustine et al., 1987). Previous studies (Brethes et al., 1987; Cazalis et al., 1987a) have analysed the relationship between $[Ca^{2+}]_i$ and the amount of AVP release. However, the time course of both the rise in $[Ca^{2+}]_i$ and the release process and in particular the temporal relationship between changes in membrane potential, $[Ca^{2+}]_i$ and exocytosis of vertebrate nerve terminals has not yet been directly investigated.

The exocytotic process involving granule-plasma membrane fusion is associated with an increase of the

terminal plasma membrane area. Because biological membranes have a rather constant specific capacitance of $\sim 1 \mu\text{F}/\text{cm}^2$ the area expansion resulting from exocytosis is associated with a proportional increase of the plasma membrane capacitance. Minute changes in membrane capacitance associated with exo- and endocytosis have been measured at very high resolution in a variety of cells using the whole-cell configuration of the patch-clamp technique (for review see Lindau, 1991). In particular, depolarization induced capacitance changes reflecting exocytotic granule fusion were demonstrated in the pioneering work of Neher and Marty (1982) on chromaffin cells. Very recently the patch-clamp technique has been applied to study ion channels (Lemos et al., 1986; Lemos and Nordmann, 1986; Lemos and Nowycky, 1989) and capacitance changes (Fidler-Lim et al., 1990) in neurosecretory nerve terminals in the whole-terminal configuration. To gain further insight into the kinetic relationships between depolarization, $[Ca^{2+}]_i$ and exocytosis we have now performed $[Ca^{2+}]_i$ measurements in single nerve terminals using fura-2 during step depolarizations. In intact terminals, these results are compared with the release of AVP from populations of nerve terminals. In single voltage clamped nerve terminals we show that the time course of the capacitance change associated with exocytosis can be

Address correspondence to Dr. Lindau.

recorded during depolarization giving a good estimate of the time course of granule fusion. With these methods the time course of $[Ca^{2+}]_i$ and exocytosis can be directly compared in the same nerve terminal. Some of these data have been presented in abstract form (Lindau and Nordmann, 1991).

MATERIALS AND METHODS

Preparation of nerve terminals

Nerve endings were isolated from Sprague-Dawley rats (200–400 g) as described (Cazalis et al., 1987b). Briefly, the pars intermedia was carefully removed and the neural lobe was homogenized in a buffer at 37°C containing 270 mM sucrose, 10 μM EGTA, 10 mM HEPES-Tris at pH 7.2. For the release experiments the homogenate was centrifuged at 100 g for 1 min and the supernatant was then centrifuged at 2,400 g for 4 min. The pellet was resuspended in physiological saline at 37°C containing (mM) 135 NaCl, 5 KHCO₃, 1 MgCl₂, 2.2 CaCl₂, 10 glucose and buffered at pH 7.2 with 10 mM HEPES-NaOH. The preparation contains mainly nerve endings having a size of 2 μm or less but also hundreds of larger ones (Nordmann and Dayanithi, 1988) which were used for the experiments described here.

AVP release experiments

The amount of nerve endings corresponding to one neural lobe was loaded onto a 0.2-μm filter (LC Acrodisk Gelman, Ann Arbor, MI) and perfused at 25 μl/min for 45 min with physiological saline. They were then perfused with normal saline in which 100 mM Na⁺ had been substituted by *N*-methyl-D-glucamine (NMG). After 15 min, the flow rate was increased progressively during the next 45 min until it reached ~25 μl/s. Stimulation of AVP release was induced by 50 mM K⁺. Osmolarity was maintained by reducing NMG accordingly. $t_{1/2}$ of the concentration change at the filter was ~4–6 s as determined with Rb⁸⁶. The experiments were done at 37°C. Fractions of 1–6 s were then collected manually and AVP was determined by radioimmunoassay as described (Cazalis et al., 1985).

$[Ca^{2+}]_i$ measurements on intact isolated terminals

The neural lobe was homogenized at 37°C in the homogenization buffer given above but containing in addition 1 mM phenylmethylsulfonyl fluoride and 100 μM benzamide. Following centrifugation, at ~2,400 g for 1.5 min the pellet was resuspended in 0.5 ml of physiological saline at 37°C containing (mM): 135 NaCl, 5 KCl, 1 MgCl₂, 2.2 CaCl₂, 10 glucose, 10 HEPES-NaOH pH 7.2. The endings were incubated for 30 min at 37°C with 3 μM fura-2/AM. After fura-2 loading, the nerve endings were again centrifuged and resuspended in the physiological saline. $[Ca^{2+}]_i$ in individual nerve endings was determined by dual wavelength microspectrofluorometry of fura-2 as described (Stuenkel, 1990). All measurements were performed at 37°C in a chamber (100-μl volume) providing rapid exchange of the superfusing physiological saline (1–1.5 ml/min). Elevated K⁺ solutions were kept isoosmotic by a similar reduction in Na⁺, the reduction in Na⁺ alone (NMG replacement) had no effect on $[Ca^{2+}]_i$. A single nerve ending was chosen using a pinhole diaphragm stopped down to a diameter of 5 μm. Alternating excitation wavelengths of 340 ± 3.8 and 380 ± 3.8 nm were used with emitted photon counts collected and

analyzed after passage through a barrier filter (510 ± 20 nm). Auto-fluorescence was determined on unloaded endings and subtracted from the signal at each wavelength before calculation of the 340/380 nm ratio and conversion to $[Ca^{2+}]_i$. The fluorescence ratio was converted to $[Ca^{2+}]_i$ using the equation of Grynkiewicz et al. (1985). Values of R_{min} , R_{max} and F_0/F_s were determined using an external standard calibration technique resulting in values of 0.77, 16.1, and 8.5 respectively. A K_d value for fura-2 of 224 nM was taken from the literature.

Patch-clamp capacitance measurements

The homogenate of the neural lobe containing the nerve terminals was transferred into a recording chamber without further purification to prevent loss of large nerve endings. After a few minutes, during which the nerve terminals were allowed to settle on the glass coverslip, which formed the bottom of the chamber, the dish was perfused with a saline containing (mM): 40 NaCl, 100 NMG-Cl, 5 KCl, 1 MgCl₂, 2.2 CaCl₂, 10 glucose buffered at pH 7.2 with 20 mM HEPES-NaOH. The internal saline (pipette solution) contained 125 mM potassium-L-glutamate, 10 mM NaCl, 4 mM MgCl₂, 2 mM Na₂ATP and 10 mM HEPES-NaOH pH 7.2–7.3 and either 100–200 μM EGTA or 100 μM fura-2. In some experiments, the external saline was diluted by ~10% with H₂O to adjust the osmolarity to be equal to that of the internal solution. All experiments were performed at room temperature (~21–24°C).

A continuous sine wave with an amplitude of ±10–20 mV was added to a given holding potential and the sum was applied as the command voltage of the patch-clamp amplifier (EPC 7, List electronics, Darmstadt, Germany) operating in the voltage clamp mode. All potentials were corrected for the liquid junction potential (~10 mV) which develops at the pipette tip when immersed into the bath solution. The current output signal was fed into an integrating two phase lock-in amplifier (Lindau and Neher, 1988; Breckenridge and Almers, 1987). At a particular phase setting, one of the two lock-in outputs (Y_2) is only sensitive to changes in membrane capacitance whereas the other output (Y_1) is only affected by changes in access resistance and membrane resistance (Lindau and Neher, 1988; Joshi and Fernandez, 1988).

We have adapted the phase tracking method (Fidler and Fernandez, 1989) for use with a conventional two phase lock-in amplifier which was set at a fixed phase. The admittance change (ΔY) in the whole-cell patch-clamp configuration due to small changes of access resistance (ΔR_A), membrane conductance (ΔG_M) and membrane capacitance (ΔC_M) is given by:

$$\Delta Y = T^2(\omega) \cdot (\Delta G_M + \Delta R_A \omega^2 C_M^2 + i\omega \Delta C_M), \quad (1)$$

(Lindau and Neher, 1988) where $T^2(\omega)$ stands for the factor

$$T^2(\omega) = 1/(1 + R_A G_M + i\omega C_M R_A)^2 = |T(\omega)|^2 \cdot e^{i\phi}. \quad (2)$$

When the phase of the lock-in is set to Φ , then the lock-in output changes ΔY_1 and ΔY_2 are directly proportional to the changes ΔC_M , ΔG_M and ΔR_A :

$$\Delta Y_1 = \Delta Y_R \sim |T(\omega)|^2 \cdot (\Delta G_M + \Delta R_A \omega^2 C_M^2) \quad (3)$$

$$\Delta Y_2 = \Delta Y_C \sim |T(\omega)|^2 \cdot \omega \Delta C_M. \quad (4)$$

Changes in R_A and G_M are shifted by 90° with respect to the C_M signal and thus do not interfere with the capacitance measurement. If the phase is shifted by a value $\Delta\Phi$ from the appropriate setting the

measured values are:

$$\Delta Y_1 = \Delta Y_R \cos(\Delta\Phi) + \Delta Y_C \sin(\Delta\Phi) \quad (5)$$

$$\Delta Y_2 = \Delta Y_C \cos(\Delta\Phi) - \Delta Y_R \sin(\Delta\Phi). \quad (6)$$

A 1 M Ω resistor was periodically switched into the connection between the bath electrode and the ground plug of the head stage to impose a defined change of R_A on the circuit. This change leads to a change in the two output signals of the lock-in amplifier depending on the phase setting:

$$\Delta Y_1 = \Delta Y_R \cos(\Delta\Phi) \quad (7)$$

$$\Delta Y_2 = -\Delta Y_R \sin(\Delta\Phi). \quad (8)$$

The changes ΔY_1 and ΔY_2 due to the imposed change of R_A thus provide the phase shift $\Delta\Phi$:

$$\Delta\Phi = -\arctan(\Delta Y_2/\Delta Y_1), \quad (9)$$

and ΔY_R and ΔY_C can subsequently be calculated from ΔY_1 and ΔY_2 :

$$\Delta Y_R = \Delta Y_1 \cos(\Delta\Phi) - \Delta Y_2 \sin(\Delta\Phi) \quad (10)$$

$$\Delta Y_C = \Delta Y_2 \cos(\Delta\Phi) + \Delta Y_1 \sin(\Delta\Phi). \quad (11)$$

The two lock-in outputs were sampled every 35 or 40 ms by a PDP 11/73 computer equipped with an A/D converter. The capacitance and conductance trace were calculated on line, shown on a graphics display and stored on disk for subsequent analysis.

Fura-2 fluorescence excited at 358 and 391 nm using a rotating filter wheel (emission wavelength 504 ± 20 nm) was measured with a photomultiplier as described [Nüsse and Lindau, 1990]. $[Ca^{2+}]_i$ was estimated as described using an apparent K_d value of 222 nM which was calculated for the internal solution used in the present experiments (Nüsse and Lindau, 1990). One ratio measurement was performed every 300–400 ms.

RESULTS AND DISCUSSION

Intact nerve terminals

To investigate the relationship between depolarization, $[Ca^{2+}]_i$ and exocytosis in intact nerve terminals, we have introduced the indicator dye fura-2 into the terminals using the ester loading method (fura-2/AM). $[Ca^{2+}]_i$ was recorded in individual terminals depolarized by perfusion with an elevated K^+ saline for 30 s (Fig. 1 a). $[Ca^{2+}]_i$ starts to increase ~ 4 s after beginning of the perfusion and then rises to a peak value of ~ 500 nM with a half time of ~ 10 s. The increase thus closely follows the exchange time of the perfusion system which has a half time of ~ 10 s. Upon returning to normal saline, $[Ca^{2+}]_i$ decreases with a half time of ~ 15 s to a level close to that observed before depolarization. Because there is no presently available technique to measure neurohormone release with high temporal resolution from a single terminal we show the time course of AVP release (Fig. 1 a) from a population of isolated nerve terminals depolarized by elevated K^+ using a rapid perfusion

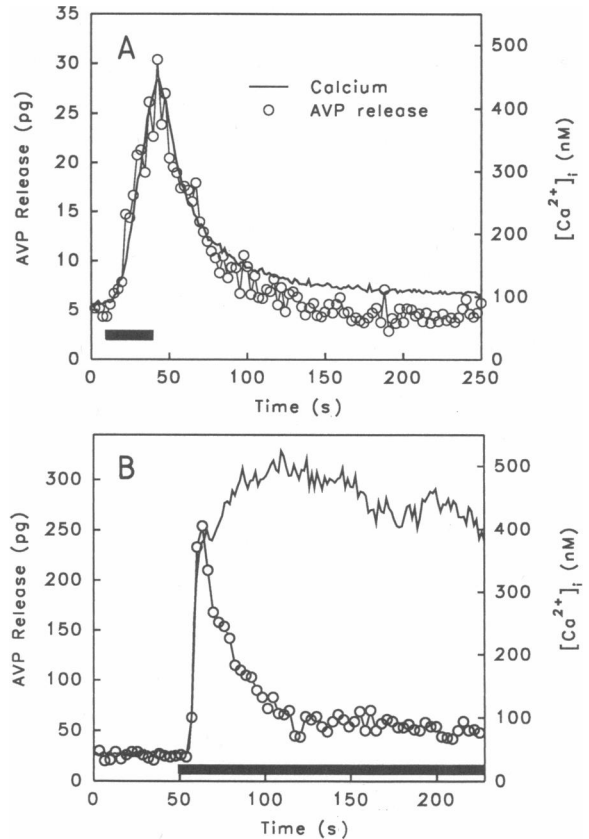
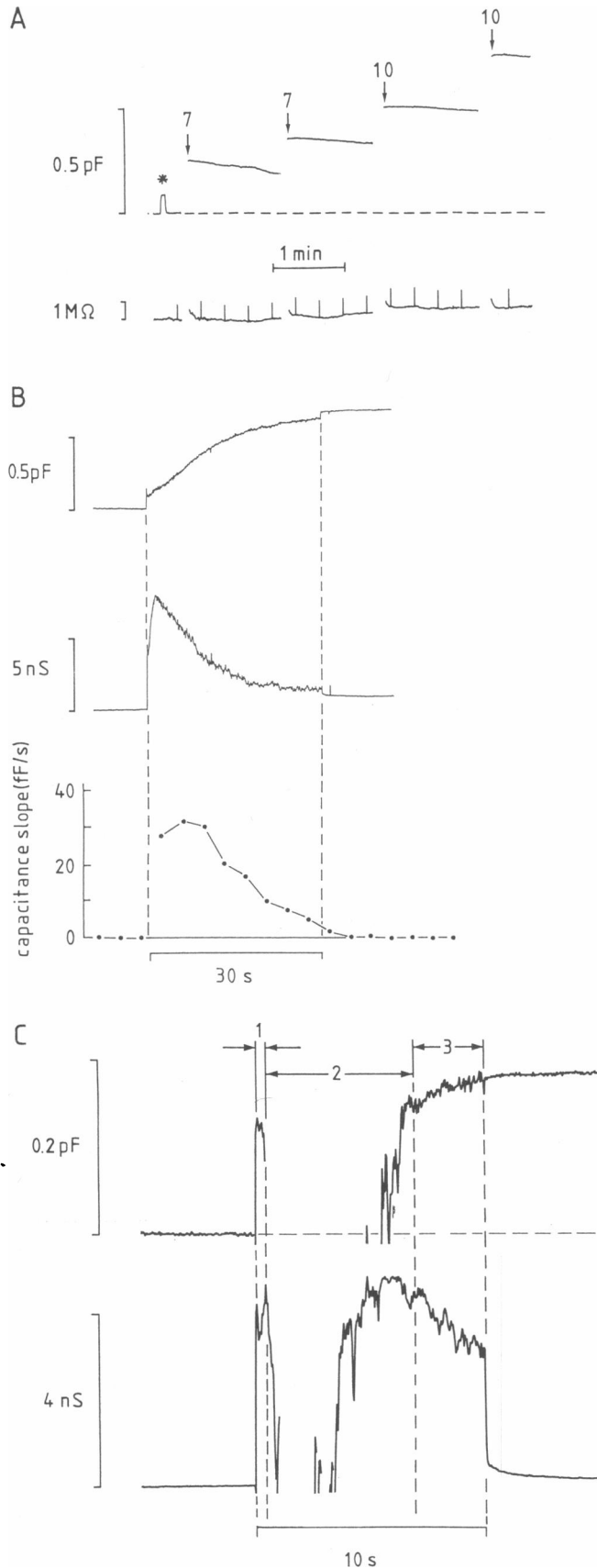


FIGURE 1 $[Ca^{2+}]_i$ and vasopressin release from isolated neurosecretory nerve endings. The nerve terminals were depolarized with 50 mM K^+ for 30 s (A) or for a prolonged period of time (B) as indicated by the heavy bars. The continuous line represents the calcium concentration in a single nerve terminal whereas the open circles represent the AVP release from a population of nerve endings. AVP contained in fractions of 2.5 s (a) and 3.5 s (b) was determined by radioimmunoassay.

system with a similar exchange half time (see Methods). Upon K^+ -induced depolarization, the rate of AVP release increases about 6-fold and the increase again follows the time course of the solution exchange. There is a striking correlation between the rise of $[Ca^{2+}]_i$ and that of the rate of release indicating that, during a 30 s depolarization period, exocytosis is controlled by $[Ca^{2+}]_i$ in a concentration dependent manner. When a terminal was depolarized by elevated K^+ for several minutes, $[Ca^{2+}]_i$ again reached ~ 500 nM after ~ 15 s but in response to sustained depolarization remained elevated during the depolarization period (Fig. 1 b). However, under these conditions AVP release which rapidly increased by about 10-fold declined to near basal levels within 60 s in spite of the sustained high $[Ca^{2+}]_i$ (Fig. 1 b). In such experiments, the amount of AVP release



evoked by 30–60 s K^+ depolarization can be estimated to be in the range of 0.6–2% of the total neuropeptide content of the nerve endings (data not shown).

Whole terminal patch-clamp experiments

The ability to directly control membrane potential in the patch-clamp whole-terminal configuration and to simultaneously monitor exocytosis by time-resolved capacitance measurements allows a more precise measurement of the relationship between these parameters. The nerve terminals which we have used for these experiments had diameters (d_T) between 5 and 10 μm and a whole-terminal capacitance of 0.7 to 3 pF. About $\frac{1}{4}$ of the intranerve terminal volume is filled with secretory granules having a mean diameter (d_G) of ~ 180 nm (Nordmann, 1977). A nerve ending thus contains $\sim \frac{1}{4} \cdot (d_T/d_G)^3$ granules which yields 6,000 to 40,000 granules being contained in each of these terminals. Assuming a specific capacitance of $1 \mu\text{F}/\text{cm}^2$ (i.e., $10 \text{ fF}/\mu\text{m}^2$) the fusion of one such granule should lead to a capacitance increase of 1 fF and for a nerve terminal with 3-pF capacitance ($d_T \sim 10 \mu\text{m}$) all the granules would sum up to a total membrane capacitance of 40 pF. The amount of capacitance increase observed in response to depolarization in individual terminals was quite variable but never exceeded a few percent of the estimated total amount of granules. When the total capacitance increase was comparatively large (> 1 pF) the appearance under the microscope changed from perfectly smooth to rough with bleblike structures. However even these terminals were still well described by the usual equivalent circuit with a single membrane capacitance C_M .

The upper trace of Fig. 2 *a* shows a recording from a nerve terminal with comparatively large exocytotic activity. The lower trace contains the changes of the access

FIGURE 2 Capacitance changes in a single nerve terminal in response to step depolarizations from a holding potential of -80 mV to a potential of -10 mV. A ± 20 mV sine wave was added to the potential throughout the recording. In (*A*) the upper trace shows capacitance changes, the lower trace shows changes in access resistance and membrane conductance. At the asterisk the capacitance compensation was transiently reduced by 0.1 pF. At the arrows the terminal was depolarized for the indicated number of seconds. Because of amplifier saturation the traces during these depolarizations were deleted. The periodic deflections in the lower trace are generated by the superimposed $1 \text{ M}\Omega$ access resistance (R_A) changes. In (*B*) the same nerve terminal was depolarized for 30 s. The top trace shows the capacitance changes, the middle trace the conductance changes and the bottom trace shows the rate of the capacitance increase. At the asterisk the capacitance compensation was transiently reduced by 0.1 pF. (*C*) The capacitance and conductance trace measured during the third depolarization on an expanded time scale. The amplifier was saturated during period 2 but not during periods 1 and 3 of depolarization.

resistance connecting the measuring electrode to the interior of the nerve terminal as well as changes of membrane conductance. The small regularly spaced deflections in the lower trace are due to the superimposed changes of the access resistance which were used to track the correct phase for the capacitance measurement. The fact that these changes in access resistance do not generate corresponding signals in the capacitance trace confirms that the phase has been determined correctly. At the beginning, the capacitance compensation was transiently reduced by 100 fF (asterisk) to ensure the correct phase setting and to provide a calibration mark for the subsequent capacitance changes. The terminal was then repeatedly depolarized from a holding potential of -80 mV to -10 mV for the indicated amount of time (in seconds) whereas the 800 Hz sine wave command voltage was added to the clamp potential throughout the experiment. During the depolarization the membrane conductance increased to such an extent in this experiment that the patch-clamp amplifier was saturated most of the time and the rising phase of the capacitance could not be recorded throughout the depolarizations. However, it can be seen that the capacitance had increased by 200–300 fF corresponding to the fusion of 200–300 granules during each depolarization. This terminal had an initial capacitance of 2.6 pF and may accordingly be assumed to contain about 30,000 granules. During a 7–10 s depolarization we thus observe fusion of $\sim 1\%$ of the granules. Note that the exocytotic capacitance increase occurred during the depolarization period and that in this experiment there was very little capacitance increase after repolarization. Similar experiments were performed on 23 terminals. Out of these only 12 terminals showed a capacitance increase exceeding 30 fF. Of interest is the preliminary observation that following prolonged depolarization with high K^+ nerve endings also show a wide range of secretory activity as measured by the amount of exocytotic vacuoles per nerve terminal. Whereas in the same sample some terminals have numerous endocytic vacuoles others show no sign of secretory activity. This suggests that under identical stimulatory conditions even intact terminals do not release in a uniform manner (Nordmann and Artault, manuscript in preparation).

Time course of exocytosis in a single nerve terminal during sustained depolarization

To determine if the exocytotic activity occurs mainly at the beginning or throughout the depolarized phase we have made an attempt to estimate the time course of exocytosis during the depolarization period. The amplifier gain was reduced and the same nerve ending was

again depolarized for 30 s. Fig. 2 *b* shows the time course of the capacitance (*top trace*) recorded before, during and after the depolarization. At the beginning of the depolarization the capacitance measurement shows a spike which is an artifact presumably due to the activation of Na^+ and K^+ channels (Thorn et al., 1991). After the initial spike, the trace indicates an elevated capacitance and during the following depolarization period a gradual capacitance increase is seen. The final capacitance change (~ 0.7 pF) is only slightly affected when the terminal is repolarized to -80 mV. The conductance (*middle trace*) immediately increases by 3.8 nS and then rises slowly until a peak conductance of 8 nS is reached after 1.3 s. The conductance subsequently declines with a half time of ~ 10 s to a value < 1 nS above the level in the hyperpolarized state. This behavior can be explained by the rapid activation of I_A (Thorn et al., 1991) followed by the activation of Ca^{2+} -activated currents (Lemos and Nordmann, 1986; Thorn and Lemos, 1988).

The activation of voltage dependent conductances will, of course, interfere with the capacitance measurements and cannot easily be accounted for in the equivalent circuit used for the analysis (Neher and Marty, 1982; Lindau and Neher, 1988). However, the capacitance value after 10 s of depolarization in the top trace of Fig. 2 *b* is 380 fF, a value very close to the capacitance increase which is expected according to the preceding 10 s depolarization indicating that the error in the capacitance trace is rather small. As mentioned above, the amplifier gain was higher during the previous 7–10 s depolarizations allowing a more accurate phase tracking. The large conductance increase initially saturated the patch-clamp amplifier but as seen in Fig. 2 *b* the conductance dropped considerably within 10 s. Fig. 2 *c* shows the capacitance and conductance trace recorded during the third depolarization on an expanded time scale. After ~ 400 ms (period 1) the conductance saturated the amplifier and for the next 6.5 s (period 2) capacitance and conductance could not be measured. During the last 3.1 s, however, the conductance was low enough such that the amplifier was not saturated any more and the capacitance trace exhibits a slow increase during this period (period 3). The final capacitance just before repolarization coincides extremely well with the level measured just after repolarization. This excellent agreement of the capacitance values at a time where the conductance was still very large demonstrates that the time course of exocytosis is not strongly distorted by voltage dependent conductances. During the first 400 ms the capacitance is already about half as large as the final value but at this time voltage and time dependent conductance changes could present a more severe problem in distorting the capacitance trace. The question if there is a rapid, comparatively large capacitance in-

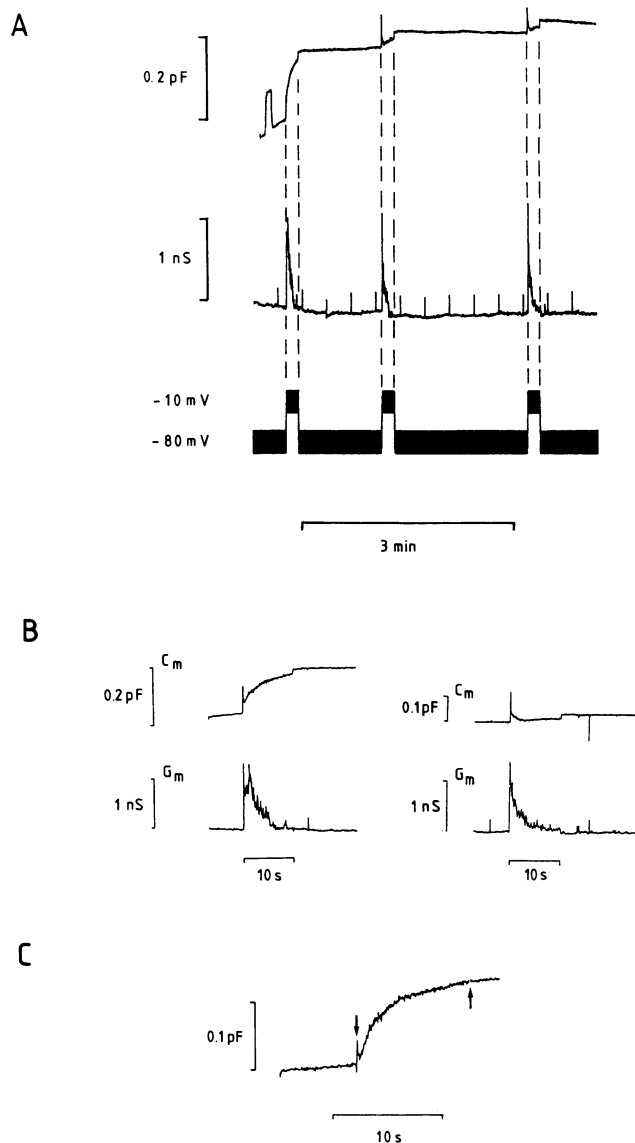


FIGURE 3 (A) Capacitance, conductance and membrane potential of a nerve terminal depolarized for 10 s three times as indicated by the dashed lines. (B) The capacitance and conductance traces of the first (left) and the third (right) depolarization on an expanded time scale. (C) The difference of the two capacitance traces shown in (B).

crease just after the onset of a step depolarization will be addressed below in more detail.

The results obtained on a different nerve terminal (Fig. 3 a) further demonstrate that the capacitance increases gradually with a decreasing slope. This terminal was depolarized three times for ~ 10 s. The first depolarization induces a gradual capacitance increase with a time course similar to that of Fig. 2 b whereas the other two depolarizations induce only much smaller

capacitance changes. In Fig. 3 b, the capacitance and conductance changes associated with the first and the third depolarization are shown on an expanded time scale. Both depolarizations induce a transient conductance increase of about 1 nS whereas the capacitance changes are quite different. Subtraction of the capacitance trace during the third depolarization from that during the first depolarization as a method to correct for conductance induced distortion is shown in Fig. 3 c. The difference rises gradually from the initial level to the final level with a decreasing slope resembling the gradual increase in the original recording of the first depolarization as well as the gradual increase seen in Fig. 2 b. It should be noted that, as in Fig. 2 c, the final capacitance trace just before repolarization matches exactly the capacitance trace after repolarization.

The results show that the capacitance measurement is only weakly distorted by the presence of voltage dependent ionic conductances. It should be kept in mind, however, that this requires a very accurate adjustment of the lock-in phase angle. A misalignment of the phase angle by 6° would reduce the capacitive signal by $< 1\%$, but would add about 10% of the conductance signal to the capacitance trace. For a peak value of 5 nS this would shift the capacitance by 100 fF. Such a projection of the conductance into the capacitance trace is quite obvious in the third depolarization of Fig. 3 (see Fig. 3 b, right). To prevent large distortions of the capacitance trace accurate phase tracking is thus of utmost importance. Because the time course of the capacitance change gives a reasonable estimate of the net increase of membrane area during depolarization, we have plotted the slope reflecting the rate of exocytotic activity in Fig. 2 b, lowest trace. It can be seen that the slope of the capacitance is 30–35 fF/s during the first 8–10 s. Because this terminal can be assumed to contain $\sim 30,000$ granules with ~ 1 fF/granule (see above) this capacitance slope corresponds to a release rate of 0.1% per second. In three other terminals of similar size the initial slope was 25–50 fF/s corresponding to release rates between 0.1 and 0.5% of the estimated total number of granules per second. After ~ 10 s, the slope drops rapidly. The rate of release is reduced to half the maximal rate ~ 15 s after the onset of depolarization and is close to zero after 30 s. The estimated fraction of granules released during the 30 s depolarization is about 2.3% which is in very good agreement with the AVP release obtained with K^+ depolarization in the intact terminals (see above). The total amount released by all the five depolarizations was $\sim 6\%$ which is also very close to what can be released by repetitive K^+ depolarization. All terminals showing a large depolarization-induced capacitance increase which was recorded for several seconds

during depolarization showed a similar time course of the capacitance increase. It should be noted that the capacitance measurement only gives the net change of the membrane area. The rate of ~ 30 fF/s would correspond to the fusion of 30 granules per second if no endocytotic membrane uptake occurs simultaneously. If stimulation induces a simultaneous activation of exocytosis and endocytosis, then AVP release could occur without inducing a measurable capacitance change. However, the similarity of the amplitude and time course with that of AVP release suggests that the capacitance increase reflects the exocytotic activity reasonably well.

Depolarization-induced $[Ca^{2+}]_i$ change in voltage clamped nerve terminals

As seen in Fig. 2 *b*, it takes more than a second until the conductance increase reaches its maximum. This behavior indicates that this part of the conductance increase may be due to Ca^{2+} dependent cation and K^+ channels which have previously been described in the nerve terminal membrane (Lemos and Nordmann, 1986; Thorn and Lemos, 1988). If the conductance decrease indicates a parallel decline of $[Ca^{2+}]_i$, this could explain a decrease in exocytotic activity (capacitance slope). However, as shown in Fig. 2 *b* the capacitance slope is rather constant for ~ 10 s whereas the conductance already decreases to half the peak value during this period of time indicating that $[Ca^{2+}]_i$ is still high enough to maintain a constant exocytotic activity.

In the whole terminal configuration, the dye fura-2 can be introduced into the nerve terminal by including it, in its salt form, in the pipette solution. The fluorescence ratio recorded from a voltage clamped nerve terminal is shown in Fig. 4. The terminal was held at -80 mV and was depolarized for 10 s to -10 mV as indicated by the time bar while the sine wave was always added to the holding potential (Fig. 4 *a*). In response to depolarization $[Ca^{2+}]_i$ increased from a resting level of ~ 100 nM to a peak level of ~ 600 nM, a value very similar to that observed in the terminals depolarized with elevated K^+ (Fig. 1) (Brethes et al., 1987; Stuenkel, 1990). $[Ca^{2+}]_i$ was measured in 10 terminals and only one showed no $[Ca^{2+}]_i$ increase in response to depolarization. The initial rise is compared with the time course of the membrane potential in Fig. 4 *b*. It can be seen that the rise in $[Ca^{2+}]_i$ lags behind the onset of depolarization. The half time in this terminal was ~ 750 ms and half times between 300 and 700 ms were observed in four other nerve terminals. The fact that the rate of release as well as $[Ca^{2+}]_i$ increased more slowly, within several seconds, in the perfusion

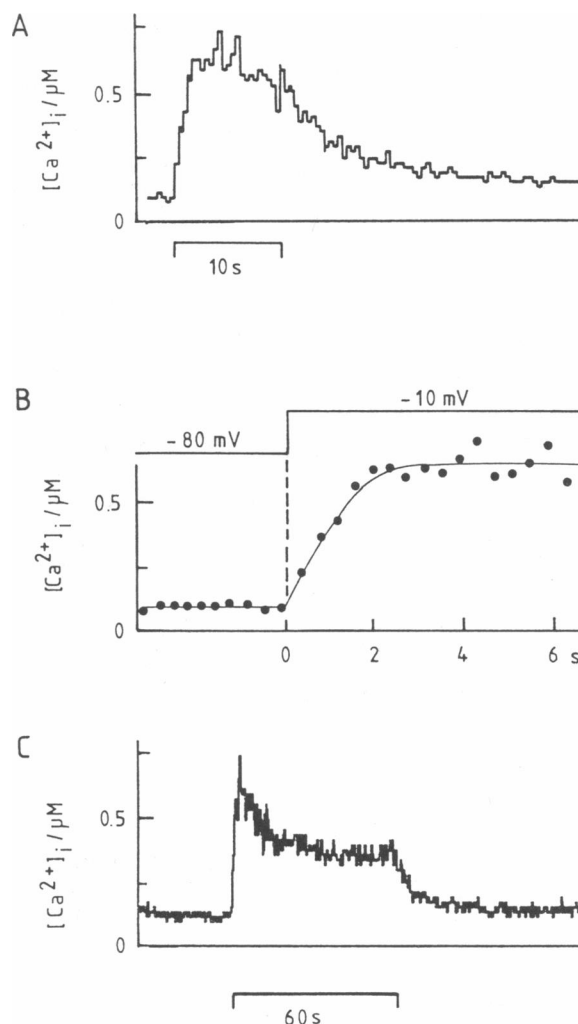


FIGURE 4 Changes of $[Ca^{2+}]_i$ measured in a single voltage clamped nerve terminal loaded with $100 \mu M$ fura-2 via the patch pipette. In (A) the nerve terminal was depolarized for 10 s as indicated by the time bar. In (B) the rise of the fluorescence ratio is shown together with the clamp potential at higher time resolution. In (C) the same nerve terminal was depolarized for 1 min.

experiment is apparently due to the slower rate of depolarization under these conditions. When the same terminal was depolarized for 1 min (Fig. 4 *c*), $[Ca^{2+}]_i$ declined somewhat after the peak was reached but remained elevated throughout the depolarization period. Sustained depolarization thus generates a maintained elevation of $[Ca^{2+}]_i$ even under voltage clamp. After repolarization $[Ca^{2+}]_i$ returned to the resting level with a half time of ~ 5 s. The steady-state $[Ca^{2+}]_i$ level during prolonged depolarization was quite variable. Whereas in some nerve endings it was very close to the initial peak level, in other nerve terminals $[Ca^{2+}]_i$ de-

clined to near the resting level with a half time of ~ 20 s during the depolarized period.

Nerve terminals of the rat neural lobe contain two types of calcium channels, a high-threshold rapidly inactivating channel (N_T -type) and a high threshold long-lasting (L -type) channel. The N_T -type channel inactivates with a time constant of ~ 30 ms and remains inactivated as long as the membrane potential is > -60 mV (Lemos and Nowycky, 1989). Because in our experiments the sine wave command voltage varied between -30 mV and $+10$ mV the N_T -type channel is expected to be inactive and is thus unable to contribute to the slow increase and the sustained elevation of $[Ca^{2+}]_i$. Fig. 4 shows that $[Ca^{2+}]_i$ rapidly returns to the resting level after repolarization indicating that the sustained elevation of $[Ca^{2+}]_i$ is associated with a sustained opening of voltage-dependent Ca^{2+} channels.

It should be mentioned that in the terminal of Fig. 4 as well as three other terminals with a similar $[Ca^{2+}]_i$ increase, no or only small capacitance changes were observed in response to the depolarization indicating that this $[Ca^{2+}]_i$ level is either insufficient to induce

exocytosis or that these terminals were insensitive to the calcium signal.

$[Ca^{2+}]_i$ and exocytosis in voltage-clamped nerve terminals

Fig. 5 *a* shows a simultaneous recording of membrane capacitance (*top trace*), membrane conductance (*middle trace*), and $[Ca^{2+}]_i$ (*bottom trace*). The nerve terminal, which had an initial capacitance of 1.9 pF was depolarized for 4 s (*horizontal bar*) which is expanded in Fig. 5 *b*. During the depolarization, $[Ca^{2+}]_i$ increased from ~ 160 nM to > 1.5 μ M. Because fura-2 approaches saturation in this concentration range the actual concentration may be even higher. The rise of $[Ca^{2+}]_i$ in this experiment is also quite slow but appears to occur in a rapid and a slow phase. While the capacitance was still increasing the depolarization was switched off and the capacitance record changed by $\sim 25\%$ presumably due to a slight misalignment of the phase setting. Because the two lock-in outputs measured at two orthogonal phases, the trace for any other phase can be calculated (see equa-

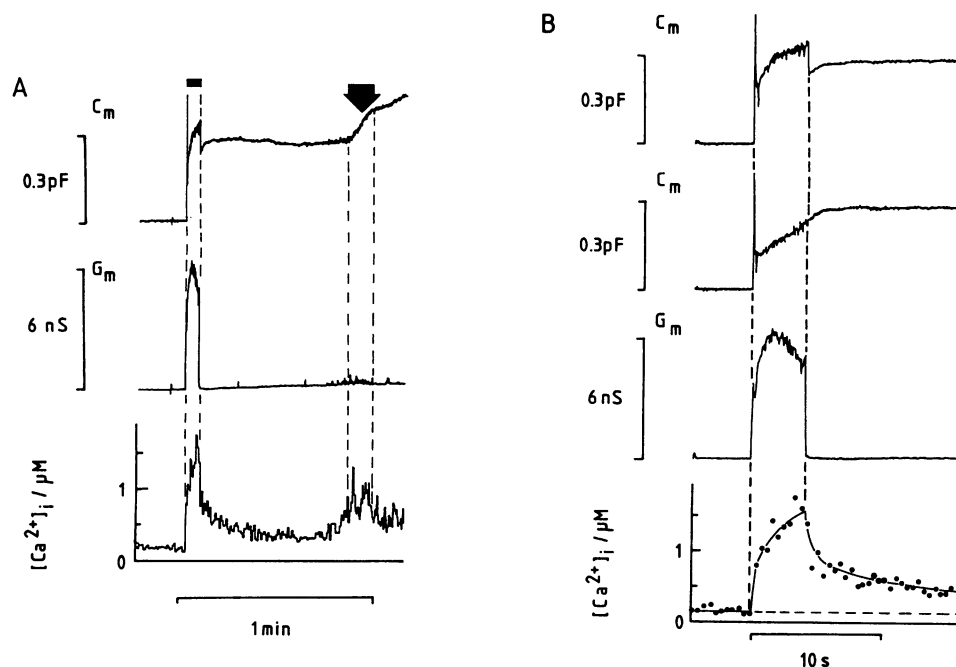


FIGURE 5 (A) Simultaneous recording of capacitance (*top trace*), conductance (*middle trace*) and the fura-2 fluorescence ratio (*bottom trace*) in a single voltage clamped nerve terminal. Holding potential was -80 mV. During 4 s, as indicated by the horizontal bar, the nerve terminal was depolarized to -10 mV. A ± 20 mV sine wave was added to the membrane potential throughout the recording. At later times conductance fluctuations are seen in the middle trace indicating a leak. During these conductance fluctuations $[Ca^{2+}]_i$ increases significantly (*arrowhead*). At the same time a correlated capacitance increase occurs (*top trace*). (B) The recordings at the 4 s depolarization shown on an expanded time scale. In addition the second trace is the reconstructed trace phase-shifted by 7° from the original capacitance trace (*top*). At this phase setting the capacitance values before and after depolarization coincide. Furthermore the capacitance slopes during and just after the depolarizing pulse are very similar.

tions 10 and 11 in Materials and Methods), we have determined the capacitance trace using variable phase shifts. When the phase is shifted by 7° , the final capacitance before repolarization and the initial capacitance after repolarization coincide (Fig. 5 *b*, *second trace*). At this phase setting the capacitance slope is constant throughout the depolarization and even after repolarization the capacitance continues to increase with the same slope for ~ 1 s. $[Ca^{2+}]_i$ increases throughout the 4 s depolarization (*bottom trace*). However, as in the experiment of Fig. 2 *b*, the conductance reaches a peak after 1.3 s and then declines demonstrating that the conductance decrease is due to inactivation rather than a decline of $[Ca^{2+}]_i$. In agreement with this observation, the large conductance Ca^{2+} dependent cation channel of the nerve terminal is only transiently activated above $1 \mu M [Ca^{2+}]_i$ (Lemos and Nordmann, 1986).

Upon repolarization $[Ca^{2+}]_i$ drops below 700 nM within 1 s and at this time the capacitance slope approaches zero (Fig. 5 *b*) indicating that $[Ca^{2+}]_i > \sim 700$ nM is required to stimulate substantial exocytosis. It should be noted that in this experiment the $[Ca^{2+}]_i$ increase was much larger than in the terminal of Fig. 4 and in parallel a much larger capacitance increase was induced. Out of the nine terminals which showed a $[Ca^{2+}]_i$ increase in response to stimulation, five had a peak value > 600 nM. The first 10 s depolarization in these five terminals induced capacitance changes of 30, 60, 100, 200, and 300 fF. The terminals with the two largest capacitance changes were the only ones with a peak $[Ca^{2+}]_i > 1 \mu M$. In the four terminals with peak $[Ca^{2+}]_i$ of 500–600 nM, the capacitance increase was 30 fF or less. The observation that in the dialysed nerve terminals $[Ca^{2+}]_i$ had to approach micromolar concentrations whereas calcium concentrations < 700 nM had little effect are in very good agreement with the previously reported calcium dependence of exocytosis in permeabilized cells where half maximal release is obtained around $1 \mu M$ (Cazalis et al., 1987a) and with the recently reported calcium sensitivity of the capacitance change in melanotrophs (Thomas et al., 1990). Depolarization alone is thus insufficient to induce exocytosis at low $[Ca^{2+}]_i$. Such high $[Ca^{2+}]_i$ values were not observed when nerve terminals were stimulated by trains of action potentials (Jackson et al., 1991), but exocytosis was not measured. $[Ca^{2+}]_i$ was also lower in intact nerve terminals where the same stimulus induces significant AVP release (Fig. 1). Although, under these conditions, not all terminals show the same morphological changes (Nordmann and Artault, manuscript in preparation) which might be due to variable $[Ca^{2+}]_i$ responses we are reluctant to view 600–700 nM as the set point for exocytosis. The calibration and background subtraction procedure always gives rise to some uncertainty in the

absolute concentration values and it is difficult to exactly compare the absolute values obtained with fura-2 using different methods on different set ups.

Note that ~ 45 s after the depolarizing pulse, a leak conductance developed in the membrane or at the pipette-membrane seal in this nerve terminal (Fig. 5 *a*, *middle trace*) as indicated by the fluctuations in the conductance trace. The nerve terminal was kept at -80 mV, but the leak current apparently carried enough Ca^{2+} into the terminal to significantly elevate $[Ca^{2+}]_i$ (*arrowhead*). When the elevation of $[Ca^{2+}]_i$ approaches $\sim 1 \mu M$, a capacitance increase is generated in the absence of depolarization demonstrating that the membrane potential changer per se does not significantly affect granule fusion. These results confirm and extend previous studies on permeabilized nerve endings (Cazalis et al., 1987a) which are unable to maintain a negative membrane potential.

Depolarizations inducing only small elevations of $[Ca^{2+}]_i$ induced no slow activation and inactivation of the conductance as shown in Figs. 2, 3, and 5, indicating that the Ca^{2+} dependent ion channels were not activated. Accordingly, in many experiments where these channels were not activated, we have never observed pronounced capacitance changes. On the other hand terminals giving a large capacitance increase also showed the slow activation of the presumably Ca^{2+} dependent conductance. These results do not necessarily indicate a role for the Ca^{2+} dependent channels in the stimulation of secretion but may reflect a parallel Ca^{2+} dependence of the ion channels and the exocytotic fusion process.

Short period of high exocytotic activity

The corrected capacitance trace of Fig. 5 *b* clearly shows an initial capacitance step which might reflect a brief period of much higher exocytotic activity and an initial step is a general feature of the capacitance recordings (see also Figs. 2, *b* and *c* and 3 *a*). Although the slowest component in the decay of the voltage-dependent Na^+ and K^+ channels is of ~ 150 -ms duration (Thorn et al., 1991) and although the Ca^{2+} dependent K^+ channels have an instantaneous voltage dependence which would be in phase with the membrane potential and should thus only affect the conductance trace, it is difficult to make sure that this initial step is not an artifact due to a possible projection of the large and rapid conductance increase. We have thus measured capacitance changes in response to short depolarizations. Fig. 6 shows the response of a nerve terminal to an 80-ms depolarization step to $+20$ mV. The capacitance increased by ~ 70 fF in agreement with a recent report (Fidler-Lim et al., 1990). To induce such an increase in 80 ms, a rate of at least

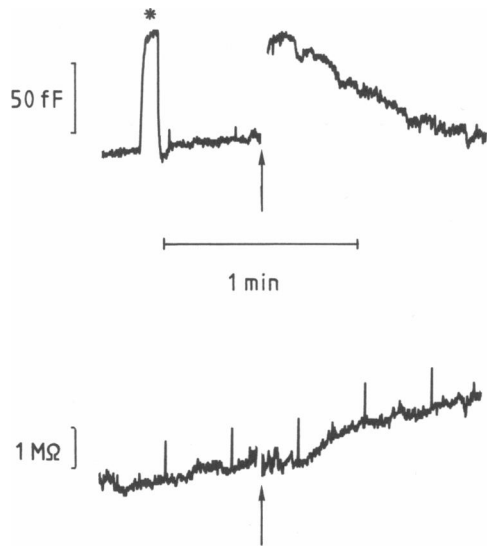


FIGURE 6 Capacitance change (*top trace*) in a nerve terminal in response to an 80-ms depolarization (*arrows*) from a holding potential of -80 mV to a potential of $+20$ mV (sine wave turned off). At the asterisk the capacitance compensation was transiently reduced by 90 fF. The sine wave was switched off during the depolarization period.

800 fF/s is required which is more than 10-fold higher than the rate measured during the later phases of prolonged depolarization. The high rate during the short depolarization and the slow increase of the capacitance during a long depolarization strongly suggests that the capacitance increase may start with an instantaneous increase with a high rate followed by a further increase at a low rate as seen in the previous continuous recordings during depolarization. Because of the uncertainties relating to possible artefacts from slight misalignment of the phase and the large conductance change during depolarization, we cannot, at present, give numbers on the proportion of terminals which show an initial step and which do not when stimulated with a long pulse.

A likely explanation for the rapid phase would be that it reflects fusion of predocked granules whereas the subsequent slow rate reflects the docking speed of further granules which, after docking, fuse immediately during the period of maintained elevation of $[Ca^{2+}]_i$. A population of docked granules had been described in chromaffin cells (Aunis et al., 1979), the related PC12 cell line (Schäfer et al., 1987) and at the presynaptic membrane of the neuromuscular junction (Heuser and Reese, 1981). The experiments presented here could thus be taken as evidence that a population of docked granules might also exist in the nerve terminals of the posterior pituitary.

Endocytosis after depolarization-induced exocytosis

After the capacitance increase Fig. 6 shows a decline of the capacitance to almost the initial level within 1 min which may reflect reuptake of the granular membranes by an endocytotic mechanism. Such a capacitance decrease is also apparent after the first depolarization of Fig. 2 *a*. Although a reuptake of granular membrane was more frequently observed after a first short depolarization rather than after massive exocytosis had occurred in response to repeated or prolonged depolarization, there was considerable variability. We have no clear explanation for this behavior but it should be kept in mind that endocytosis might require certain cytoplasmic components which may be washed out by the patch pipette and that endocytosis might require higher temperature.

Conclusions

We have measured the time course of K^+ depolarization-induced changes of $[Ca^{2+}]_i$ and AVP release on the time scale of seconds and we have demonstrated that the relationships between depolarization, $[Ca^{2+}]_i$ and exocytosis can be investigated by simultaneous time resolved recording of fura-2 fluorescence and membrane capacitance even during depolarization.

Step depolarization of a nerve terminal induces a sustained elevation of $[Ca^{2+}]_i$ which may last for many seconds or even minutes. This behavior is observed in intact nerve terminals depolarized by elevated K^+ concentrations as well as voltage clamped intracellularly dialyzed nerve terminals in the patch-clamp whole-terminal configuration. On the time scale of seconds, the increase of $[Ca^{2+}]_i$ parallels the release of neurohormone as measured by AVP release indicating that in intact terminals the rate of exocytosis is directly related to $[Ca^{2+}]_i$. However, during prolonged depolarization exocytotic granule fusion starts to cease whereas $[Ca^{2+}]_i$ remains elevated. This termination of exocytosis is not due to depletion of granules because even under optimal conditions, only fusion of a few percent of the total amount of granules can be induced and only a few percent of the total AVP can be released.

$[Ca^{2+}]_i$ entering a terminal via a leak conductance is also able to stimulate exocytosis in the absence of depolarization confirming that the change in membrane potential per se is not essential in mediating exocytotic granule fusion in the nerve terminals as previously indicated by experiments on permeabilized nerve terminals (Cazalis et al., 1987*a*). Our results extend these experiments demonstrating that exocytosis commences at the same $[Ca^{2+}]_i$ regardless of the membrane being hyperpolarized or being depolarized as is always the

case in the permeabilized terminals. On the other hand we have shown that depolarization at low $[Ca^{2+}]_i$ is insufficient to induce exocytosis.

Under voltage clamp conditions, the slow capacitance increase is preceded by a rapid phase which reflects fusion at much higher rates for a sub-second period. This rapid phase may reflect exocytosis of docked granules which have so far been observed at the presynaptic membrane of the neuromuscular junction (Heuser and Reese, 1981), chromaffin cells (Aunis et al., 1979) and PC12 cells (Schäfer et al., 1987), whereas fusion during the slow phase may be rate limited by the arrival of further granules at the plasma membrane. Our results suggest that a population of docked granules may also exist in neuroendocrine nerve terminals.

A rapid phase of exocytosis occurs in <100 ms whereas the elevation of bulk $[Ca^{2+}]_i$ extends over hundreds of milliseconds which could be taken as evidence that the calcium requirement for the rapid phase is comparatively low. It should be kept in mind, however, that in the experiments shown here $[Ca^{2+}]_i$ is only measured as the average concentration throughout the nerve terminal. Although $[Ca^{2+}]_i$ may be assumed to equilibrate very rapidly in a small nerve terminal, it should be considered that the prolonged depolarization induces a sustained influx of Ca^{2+} and the rise in $[Ca^{2+}]_i$ will thus be determined by reaching equilibrium conditions with respect to Ca^{2+} influx, efflux and buffering. Consequently, the rise at the membrane may be much more rapid than the rise of the bulk $[Ca^{2+}]_i$ throughout the terminal as recently shown for nicotinic stimulation (O'Sullivan et al., 1990) and voltage clamp depolarization (Augustine and Neher, 1990) of chromaffin cells. The apparent discrepancy between the instantaneous rapid capacitance increase and the slow rise of $[Ca^{2+}]_i$ indicates that in nerve terminals of the posterior pituitary $[Ca^{2+}]_i$ rises much more rapidly directly at the fusion sites and that the local calcium increase may be sufficient to induce exocytosis. Simultaneous capacitance and fura-2 measurements, possibly in conjunction with imaging technique providing both temporal and spatial resolution and measurements of calcium currents will provide a unique tool for detailed investigations of the relationships between depolarization, voltage-dependent Ca^{2+} channels and exocytotic granule fusion in nerve terminals.

We wish to thank Wolf Almers, Julio Fernandez, José (Pedro) Lemos and Erwin Neher for critically reading of the manuscript and valuable discussions. We also wish to thank Stefanie Wolgast for excellent technical assistance.

This work has been supported by grants from the Deutsche Forschungsgemeinschaft (DFG Sfb 312/B6, Manfred Lindau), from Rackham at the University of Michigan (Edward L. Stuenkel) and from the

Ministère de la Solidarité, de la Santé et de la Protection Sociale and from Institute de Recherches Scientifique sur les Boissons (Jean J. Nordmann).

Received for publication 1 May 1991 and in final form 22 August 1991.

REFERENCES

- Augustine, G. J., M. P. Charlton, and S. J. Smith. 1987. Calcium action in synaptic transmitter release. *Annu. Rev. Neurosci.* 10:633–693.
- Augustine, G. J., and E. Neher. 1990. Imaging calcium transients in patch clamped chromaffin cells. *Soc. Neurosci. Abstr.* 16:1013a. (Abstr.)
- Aunis, D., J. E. Hesketh, and G. Devilliers. 1979. Freeze fracture study of the chromaffin cell during exocytosis: evidence for connections between the plasma membrane and secretory granules and for movements of plasma membrane-associated particles. *Cell Tissue Res.* 197:433–441.
- Breckenridge, L. J., and W. Almers. 1987. Currents through the fusion pore that forms during exocytosis of a secretory vesicle. *Nature (Lond.)* 328:814–817.
- Brethes, D., G. Dayanithi, L. Letellier, and J. J. Nordmann. 1987. Depolarization-induced Ca^{2+} increase in isolated neurosecretory nerve terminals measured with Fura-2. *Proc. Natl. Acad. Sci. USA.* 84:1439–1443.
- Cazalis, M., G. Dayanithi, and J. J. Nordmann. 1985. The role of patterned burst and interburst interval on the excitation-coupling mechanism in the isolated rat neural lobe. *J. Physiol.* 369:45–60.
- Cazalis, M., G. Dayanithi, and J. J. Nordmann. 1987a. Requirements for hormone release from permeabilized nerve endings isolated from the rat neurohypophysis. *J. Physiol. (Lond.)* 390:71–91.
- Cazalis, M., G. Dayanithi, and J. J. Nordmann. 1987b. Hormone release from isolated nerve endings of the rat neurohypophysis. *J. Physiol.* 390:55–70.
- Dayanithi, G., N. Martin-Moutot, S. Barlier, D. A. Colin, M. Kretz-Zaepfel, F. Couraud, and J. J. Nordmann. 1988. The calcium channel antagonist ω -conotoxin inhibits secretion from peptidergic nerve terminals. *Biochim. Biophys. Res. Commun.* 156:255–262.
- Fidler, N., and J. M. Fernandez. 1989. Phase tracking: an improved phase detection technique for cell membrane capacitance measurements. *Biophys. J.* 56:1153–1162.
- Fidler-Lim, N., M. C. Nowycky, and R. J. Bookman. 1990. Direct measurement of exocytosis and calcium currents in single vertebrate nerve terminals. *Nature (Lond.)* 344:449–451.
- Grynkiwicz, G., M. Poenie, and R. Y. Tsien. 1985. A new generation of Ca^{2+} indicators with greatly improved fluorescence properties. *J. Biol. Chem.* 260:3440–3450.
- Heuser, J. E., and T. S. Reese. 1981. Structural changes after transmitter release at the frog neuromuscular junction. *J. Cell Biol.* 88:564–580.
- Jackson, M. B., A. Konnerth, and G. J. Augustine. 1991. Action potential broadening and frequency-dependent facilitation of calcium signals in pituitary nerve terminals. *Proc. Natl. Acad. Sci. USA.* 88:380–384.
- Joshi, C., and J. M. Fernandez. 1988. Capacitance measurements: an analysis of the phase detector technique used to study exocytosis and endocytosis. *Biophys. J.* 53:885–892.

- Lemos, J. R., and J. J. Nordmann. 1986. Ionic channels and hormone release from peptidergic nerve terminals. *J. Exp. Biol.* 124:53–72.
- Lemos, J. R., J. J. Nordmann, I. M. Cooke, and E. L. Stuenkel. 1986. Single channels and ionic currents in peptidergic nerve terminals. *Nature (Lond.)* 319:410–412.
- Lemos, J. R., and M. C. Nowycky. 1989. Two types of calcium channels coexist in peptide-releasing vertebrate nerve terminals. *Neuron* 2:1419–1426.
- Lindau, M. 1991. Time-resolved capacitance measurements: monitoring exocytosis in single cells. *Quart. Rev. Biophys.* 24:75–101.
- Lindau, M., and E. Neher. 1988. Patch-clamp techniques for time-resolved capacitance measurements in single cells. *Pfluegers Arch. (Eur. J. Physiol.)* 411:137–146.
- Lindau, M., and J. Nordmann. 1991. Capacitance and calcium changes during exo- and endocytosis in single vertebrate nerve terminals. *Biophys. J.* 59:276a. (Abstr.)
- Neher, E., and A. Marty. 1982. Discrete changes of cell membrane capacitance observed under conditions of enhanced secretion in bovine adrenal chromaffin cells. *Proc. Natl. Acad. Sci. USA* 79:6712–6716.
- Nordmann, J. J. 1977. Ultrastructural morphometry of the rat neurohypophysis. *J. Anat.* 132:213–218.
- Nordmann, J. J., and G. Dayanithi. 1988. Release of neuropeptides does not only occur at nerve terminals. *Biosci. Rep.* 8:471–483.
- Nüsse, O., and M. Lindau. 1990. GTP γ S-induced calcium transients and exocytosis in human neutrophils. *Biosci. Rep.* 10:93–103.
- O'Sullivan, A. J., T. R. Cheek, R. B. Morton, M. J. Berridge, and R. D. Burgoyne. 1989. Localization and heterogeneity of agonist-induced changes in cytosolic calcium concentration in single bovine adrenal chromaffin cells from video imaging of fura-2. *EMBO (Eur. Mol. Biol. Organ.) J.* 8:401–411.
- Schäfer, T., O. U. Karli, F. E. Schweizer, and M. M. Burger. 1987. Docking of chromaffin granules: a necessary step in exocytosis? *Biosci. Rep.* 7:269–279.
- Stuenkel, E. L. 1990. Effects of membrane depolarization on intracellular calcium in single nerve terminals. *Brain Res.* 529:96–101.
- Thomas, P., A. Surprenant, and W. Almers. 1990. Cytosolic Ca²⁺, exocytosis and endocytosis in single melantrophs of the rat pituitary. *Neuron* 5:723–733.
- Thorn, P. J., and J. R. Lemos. 1988. Ca-activated K-channel in rat neurohypophysial nerve terminals. *Soc. Neurosci. Abstr.* 14:641a. (Abstr.)
- Thorn, P. J., X. Wang, and J. R. Lemos. 1991. A fast, transient K⁺ current in neurohypophysial nerve terminals of the rat. *J. Physiol.* 432:313–326.